Intracellular expression of reactive oxygen species-generating NADPH oxidase NOX4 in normal and cancer thyroid tissues

Urbain Weyemi[1,2,3], Bernard Caillou[3]*, Monique Talbot[1,3], Rabii Ameziane-El-Hassani[1,4], Ludovic Lacroix[3], Odile Lagent-Chevallier[1,2,3], Abir Al Ghuzlan[3], Dirk Roos[5], Jean-Michel Bidart[2,3], Alain Virion[1,2,3], Martin Schlumberger[2,3] and Corinne Dupuy[1,2,3]*

[1]CNRS, FRE2939, Villejuif F-94805, France
[2]University Paris-Sud 11, Orsay F-91400, France
[3]Institut Gustave Roussy, FRE2939 CNRS, 39 rue Camille Desmoulins, Villejuif F-94805, France
[4]UBRM, Centre National de l'Energie, des Sciences et des Techniques Nucléaires, Rabat M-10001, Morocco
[5]Sanquin Research, and Landsteiner Laboratory, Academic Medical Centre, University of Amsterdam, Amsterdam NL-1006, The Netherlands

(Correspondence should be addressed to C Dupuy at Institut Gustave Roussy, FRE2939 CNRS; Email: dupuy@igr.fr)

*(U Weyemi and B Caillou contributed equally to this work)

Abstract

NADPH oxidase 4 (NOX4) belongs to the NOX family that generates reactive oxygen species (ROS). Function and tissue distribution of NOX4 have not yet been entirely clarified. To date, in the thyroid gland, only DUOX1/2 NOX systems have been described. *NOX4* mRNA expression, as shown by real-time PCR, was present in normal thyroid tissue, regulated by TSH and significantly increased in differentiated cancer tissues. TSH increased the protein level of NOX4 in human thyroid primary culture and NOX4-dependent ROS generation. NOX4 immunostaining was detected in normal and pathologic thyroid tissues. In normal thyroid tissue, staining was heterogeneous and mostly found in activated columnar thyrocytes but absent in quiescent flat cells. Papillary and follicular thyroid carcinomas displayed more homogeneous staining. The $p22^{phox}$ protein that forms a heterodimeric enzyme complex with NOX4 displayed an identical cellular expression pattern and was also positively regulated by TSH. ROS may have various biological effects, depending on the site of production. Intracellular NOX4–$p22^{phox}$ localization suggests a role in cytoplasmic redox signaling, in contrast to the DUOX localization at the apical membrane that corresponds to an extracellular H_2O_2 production. Increased NOX4–$p22^{phox}$ in cancer might be related to a higher proliferation rate and tumor progression but a role in the development of tumors has to be further studied and established in the future.

Endocrine-Related Cancer (2010) **17** 27–37

Introduction

Reactive oxygen species (ROS) are highly reactive O_2 metabolites, including superoxide radical ($O_2^{\cdot-}$) and hydrogen peroxide (H_2O_2). ROS were first considered as toxic byproducts resulting in oxidative stress and damaging to biomolecules, but some early studies revealed their physiological properties (Lambeth 2007). Until 1999, the NADPH oxidase (NOX) of phagocytes was the only enzymatic system known to produce $O_2^{\cdot-}$ and H_2O_2 (Babior 1999). This enzyme, which consists of a large β-subunit termed NOX2, formerly known as $gp91^{phox}$, and a 22 kDa α-subunit ($p22^{phox}$), is involved in bacterial killing. To date, six homologs of NOX2 have been discovered, which are expressed in many tissues and constitute a new family of enzymes called NOX/DUOX (Bedard & Krause 2007). The different localizations of NOX/DUOX at the tissue, cellular and/or subcellular levels also appear related to their various functions (Babior 1999, Bedart & Krause 2007, Lambeth 2007).

DOI: 10.1677/ERC-09-0175
1351–0088/10/017–027

DUOX genes are strongly expressed in the thyroid gland, and DUOX proteins are located at the apical membrane of the thyrocytes (Dupuy *et al*. 1999, De Deken *et al*. 2000). DUOX2 generates the H_2O_2 in the extracellular colloid space that is used by the thyroid peroxidase (TPO) to organify iodide, whereas the role of DUOX1 is still unknown. Up to now, these two DUOX proteins were the only H_2O_2 generating systems described in this tissue.

ROS production has already been demonstrated in rat thyroid cells (Pomerance *et al*. 2000), but for the above mentioned reasons this production cannot be explained by the activity of DUOX1 and 2, suggesting the existence of other ROS-producing systems.

$p22^{phox}$, a subunit functionally associated with NOX1, NOX2, NOX3 and NOX4, was shown to co-immunoprecipitate with DUOX proteins in human thyrocytes, suggesting that it could also constitute a partner of these H_2O_2-generating systems (Wang *et al*. 2005). However, co-transfection experiments showed that $p22^{phox}$ had no effect on DUOX activity, suggesting that $p22^{phox}$ might not interact with DUOX but rather with another NOX that might also be expressed in the thyroid tissue (Ameziane-El-Hassani *et al*. 2005).

In this study, we demonstrate the expression of NOX4 in normal and cancer thyroid tissues that may be a H_2O_2 generator located inside the thyroid cell. NOX4 expression is increased by TSH stimulation, suggesting a role of ROS in TSH signaling.

Materials and methods

Reverse transcription and PCR

Total RNA from cells was extracted with Trizol reagent (Invitrogen, Inc.) according to the manufacturer's instructions. Total RNA (1 μg) was reverse transcribed using 10 U Superscript III transcriptase (Invitrogen) in 20 μl PCR buffer according to the manufacturer's protocol for 60 min at 55 °C. cDNA was then amplified by 30 temperature cycles (95 °C, 30 s; 60 °C, 10 s; 72 °C, 1 min) in a GeneAmp 9600 apparatus and AmpliTaq Gold's protocol (Applied Biosystems, Foster City, CA, USA). Selected primers are listed in Table 1.

Tissue samples and real-time RT-PCR

Eighty-nine frozen thyroid tissue samples stored in liquid nitrogen were selected after histological analysis and classification according to World Health Organization recommendations, as previously described (Lacroix *et al*. 2005). Tissues were collected at Institut Gustave Roussy, and informed consent was obtained from all patients. The tissue collection included 15 follicular thyroid adenomas (FTA), 26 follicular thyroid carcinomas (FTC), 19 papillary thyroid carcinomas (PTC), 4 anaplastic thyroid carcinomas (ATC), and 25 nontumoral contralateral thyroid tissues obtained from patients with a unifocal tumor and considered as normal

Table 1 Forward (sense) and reverse (antisense) oligonucleotides

NOX	Sense	Sequence 5′–3′	Size of PCR product (bp)
NOX1	+	ACAAATTCCAGTGTGCAGACCAC	371
	−	AGACTGGAATATCGGTGACAGCA	
NOX2	+	GGGCTGTTCAATGCTTGTGGCT	389
	−	ACATCTTTCTCCTCATCATGGTGC	
NOX3	+	GGATCGGAGTCACTCCCTTCGCTG	435
	−	ATGAACACCTCTGGGGTCAGCTGA	
NOX4	+	GGTGCTATTCCTCATGATCAC	299
	−	AATCTGGGCTCTTCCATACAAA	
NOX5	+	ATCAAGCGGCCCCCTTTTTTTCAC	215
	−	CTCATTGTCACACTCCTCGACAGC	
PAX8	+	CCT TTG TGA ATG GCA GAC CT	375
	−	TAG GGA GGT TGA ATG GTT GC	
TSHR	+	CTT GCT GGA CGT GTC TCA AA	418
	−	CTG GCC AAA ACC AAT GAT CT	
TPO	+	CGG GTC ATC TGT GAC AAC AC	448
	−	CGG AGT CTA CGC AGG TTC TC	
TG	+	AGG CCC TGC TCT CTA ACT CC	445
	−	GCC AAA GGA GTG CTG AAG TC	
NIS	+	CTCCCTGCTAACGACTCCAG	412
	−	GACCACCATCATGTCCAACA	

+/− Means that the oligonucleotide is sense or antisense relative to cDNA.

tissues based on histological examination (including 15 paired samples with 2 FTA, 3 FTC, 9 PTC, and 1 ATC).

Total RNA was extracted from frozen tissue samples with Trireagent (Sigma–Aldrich) and then purified on Rneasy columns (Qiagen) according to the manufacturer's protocols. Quality of RNA preparation, based on the 28S/18S rRNAs ratio, was assessed with the RNA 6000 Nano Lab-On-chip (Agilent Technologies, Palo Alto, CA, USA). One microgram of total RNA was reverse transcribed by Moloney murine leukemia virus reverse transcriptase in the presence of random primers as previously described (Applied Biosystems).

Oligonucleotide primers and Taqman probes specific for the NOXes, including NOX4 and $p22^{phox}$, were designed to be intron spanning by the Primer-Express computer software (Applied Biosystems). Sequences were obtained from the GenBank database, and the oligonucleotides were purchased from MWG Biotech (Courtaboeuf, France); these sequences are available on demand. Primers and probes for 18S were obtained from Assays-On-Demand (Applied Biosystems). Q-PCRs were performed on the equivalent of 10 ng total RNA per tube in a final volume of 18 µl (Lacroix *et al*. 2005). Each primers and probes have been controlled not to cross-react, to avoid amplification dimmers, and to provide optimal amplification efficiency tested with standard curves constructed from pool of cDNA from several tissues and cell lines that were serially diluted in nuclease-free H_2O. The intra-assay coefficient of variation was $<1\%$. Because the conventional use of a single gene for normalization leads to relatively large errors, normalization and relative mRNA expression was assessed by averaging of three internal control genes carefully selected as previously published (Vandesompele *et al*. 2002). Three housekeeping genes, 18S, ribosomal protein large P0 and cyclophilin A (PPIA), have been previously validated as internal control genes in thyroid tissues (Lacroix *et al*. 2005). A calibrator was constituted from pool of several thyroid tissues and cell lines were used as $1\times$ sample, and all other relative levels of expression were expressed as x-fold difference relative to this calibrator.

The expression levels of NOX4 and $p22^{phox}$, observed in the various groups of tumor tissues, were compared with those in normal samples by the nonparametric Mann–Whitney test. Differences in gene expression levels in paired tissue samples were analyzed by a nonparametric Wilcoxon matched pairs test. All *P* values are two sided.

Cultured cells

Primary human cells were cultured as previously described (Duthoit *et al*. 2001). Briefly, the tissue (3–4 g) was dissected free from connective tissue and minced into small fragments. The tissue fragments were washed into Coon's modification of Ham's F-12 medium (Sigma–Aldrich) containing 2.6 g/l Na_2CO_3 (Merck), penicillin/streptomycin (100 µg/ml; Invitrogen), and kanamycin (100 µg/ml; Invitrogen). To separate the epithelial cells from the connective tissue, the fragments were digested with collagenase I (100 U/ml) (Invitrogen) and the neutral protease dispase II (2.4 U/ml) (Roche Applied Science) in 20 ml of calcium- and magnesium-free PBS, pH 7.4, at 37 °C for 35 min. The digested tissue was filtered through sterile gauze swabs. Medium was added and the cells were washed by successive centrifugations at 200 ***g*** for 5 min. Finally, the cells were counted and seeded to a density of 5×10^5 cells per well in six-well plates in a final volume of 2 ml culture medium (Ham's F-12) supplemented with 5% (v/v) FCS (PAA Laboratories, Pasching, Austria), 2 mM L-glutamine (Invitrogen), 1% nonessential amino acids (PAA Laboratories), and six nutritional factors (6H medium): 1 U/l bovine TSH (Sigma–Aldrich); 10 mg/l human insulin (Roche Applied Science); 10 µg/l somatostatin (Sigma–Aldrich); 6 mg/l human transferring (Roche Applied Science); 10^{-8} M hydrocortisone (Roche Applied Science); and 10 µg/l glycyl-histidyl-lysine acetate (Sigma–Aldrich). The cells were cultured at 37 °C in a humidified air atmosphere containing 5% CO_2. The primary cultures of thyroid cells formed a confluent monolayer within 7–9 days. Primary human cells prepared in these conditions were previously shown to organify iodide (Duthoit *et al*. 2001).

Transfection of small interfering RNAs

Seventy-two hours after TSH starvation, primary human thyrocytes were transfected at 60% confluence with small interference RNA (siRNA; siNOX4 from Dharmacon, Chicago, IL, USA; SiGENOME, SMART-pool) or scrambled siRNA control (Dharmacon) by using the Jet Pei transfection reagent (Polyplus, New York, NY, USA). A pool of four different siRNAs for NOX4 was used; the target sequences were: 1) ACUAUGAUAUCUUCUGGUA; 2) GAAAUUA-UCCCAAGCUGUA; 3) GGGCUAGGAUUGUGU-CUAA; 4) GAUCACAGCCUCUACAUAU. Primary human thyrocytes were incubated for 8 h with the siRNA–Jet Pei complexes in TSH-free 5-hormone

medium (5H); 1 mU/ml TSH was then added to the medium for 48 h as required. The knockdown efficiency was checked by real-time QPCR.

Measurement of intracellular ROS

Intracellular ROS levels were measured by flow cytometry in cells loaded with the redox-sensitive dye 2′,7′-dichlorofluorescin diacetate (DCFH-DA; Invitrogen Molecular probe). The nonfluorescent DCFH-DA readily diffuses into the cells, where it is hydrolyzed to the polar derivative DCFH, which is oxidized in the presence of H_2O_2 to the highly fluorescent DCF. Approximately 5×10^5 cells were harvested by trypsinization, resuspended in 0.5 ml culture medium (Ham's F-12) supplemented with 0.2% (v/v) FCS and incubated with 10 μM DCFH-DA for 30 min in the dark at 37 °C. Fluorescence was recorded on FL-1 channel of FACScan (Becton Dickinson, Le pont-de-Claix, France).

Western blots

Human thyrocytes were washed twice with PBS and directly solubilized in denaturing sample buffer (Tris/HCl 10 mM pH 7, 2.5% (w/v) SDS, 1 mM EDTA, 1 mM EGTA, 4 M urea and protease inhibitors (0.1 mM phenylmethylsulphonyl fluoride, 5 μg/ml aprotinine, 5 μg/ml leupeptine, 157 μg/ml benzamidine and 1 μg/ml pepstatine)). Protein samples (20 μg) supplemented with 2.5% (w/v) β-mercaptoethanol and 10% glycerol were sonicated for 15 s and denatured at 70 °C during 10 min. They were then subjected to SDS-PAGE on a 4–12% acrylamide slab minigel (NUPAGE, Invitrogen) and electrotransferred to 0.2-μm Protan BA 83 nitrocellulose sheets (Schleicher & Schuell, Mantes La Ville, France) for immunodetection. Antibody directed against the human NOX4 primary antibody was purchased from Novus Biologicals (Littleton, CO 80160, USA), and its specificity was tested with crude extracts prepared from HEK293 cells transiently transfected with the vector pcDNA3.1 containing or not human NOX4. Human thyroperoxidase was immunodetected as previously described (Ameziane-El-Hassani *et al*. 2005). Immune complexes were detected with HRP-coupled goat anti-rabbit IgG antibody (SouthernBiotech, Birmingham, AL 35260, USA)

Immunohistochemistry

Forty-one thyroid samples were obtained from patients who underwent surgery at Institut Gustave Roussy. Informed consent was obtained from all patients. These samples included normal thyroid tissue ($n=8$); nodular and/or diffuse hyperplasia ($n=11$); follicular adenoma ($n=4$); papillary carcinoma ($n=11$); follicular carcinoma ($n=3$); and poorly differentiated follicular carcinoma ($n=4$).

Immunohistochemical studies were performed on formaldehyde-fixed, paraffin-embedded tissues, as previously described (Caillou *et al*. 2001). Briefly, 5-micron sections were deparaffinized. Endogenous peroxidase activity was quenched by incubation in 0.03% hydrogen peroxide, in 0.1 mol/l Tris–HCl buffer 1× (pH 7.6) for 5 min. Microwave/pressure cooker pretreatment was performed in 1 mmol/l EDTA buffer (pH 8). Sections were subsequently incubated for 60 min at room temperature with the rabbit polyclonal anti-NOX4 antiserum (1:100), with the anti-DUOX antiserum (1:100 dilution) (Caillou *et al*. 2001) that cross-reacted with DUOX1 and DUOX2 proteins (Morand *et al*. 2003), with the anti-Na/I symporter (NIS) serum (1:500) (Caillou *et al*. 2001), with the monoclonal anti-CD34 (NOVO/MENARINI; clone QB END/10; dilution: 1:60), and with the monoclonal anti-human-$p22^{phox}$ (1: 50) (mouse monoclonal antibody 449, Verhoeven *et al*. 1989). Sections were then washed in Tris–HCl 1× buffer for 5 min and incubated with a peroxidase-conjugated goat anti-rabbit antibody for 30 min (ENVISION; DAKO Corp., Carpinteria, CA, USA). After further washes, peroxidase staining was revealed in diaminobenzidine tetrahydrochloride (Polysciences Inc., Warrington, PA, USA) with 0.1% (w/v) of hydrogen peroxide, in Tris buffer, 0.01 mol/l (pH 7.2). Sections were counterstained and mounted. Negative controls were obtained by replacing the specific primary antibody by an irrelevant antibody. Kidney tissue was used as positive controls for NOX4 antibody (Shiose *et al*. 2001).

The percentage of positively stained cells was assessed semiquantitatively, being 0–25; 25–50; 50–75; or 75–100%, as well as the intensity of staining in NOX4-positive cells.

Statistical analysis

The tests were performed using the GraphPadInstat software (La Jolla, CA, USA) for ANOVA, Student *t*-test with the level of significance set at $P<0.05$.

Results

NOX mRNAs expression was analyzed by RT-PCR in normal human thyroid tissue and in human thyrocytes in culture (Fig. 1). All NOX genes, except *NOX3* gene, were expressed in the thyroid tissue. NOX2, referred to as the phagocyte NOX, was detected in thyroid tissues and is known to be expressed in phagocytic cells and endothelial cells. The expression levels of *NOX1* and

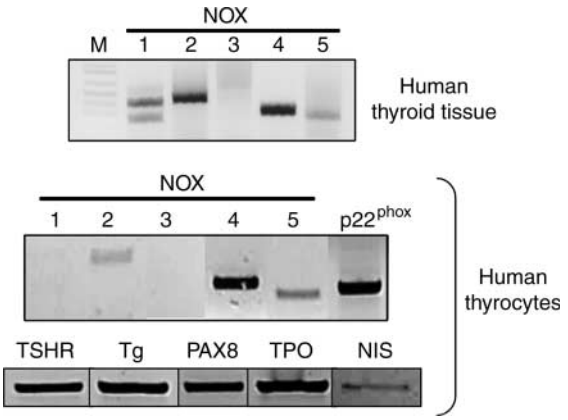

Figure 1 Expression of NOX in normal human thyroid tissues and in cultured human thyrocytes, as determined by RT-PCR. Lane M, DNA size markers; lane 1, NOX1; lane 2, NOX2; lane 3, NOX3; lane 4, NOX4 and lane 5, NOX5. Expression of thyroid-specific gene transcripts in human thyrocytes is also reported as internal controls.

NOX5 mRNAs were low in thyroid tissues, and may be derived from lymphocytes and endothelial cells (Bedard & Krause 2007). In thyrocytes in primary culture, *NOX5* mRNA was also detected at a low level but only *NOX4* and $p22^{phox}$ mRNAs were detected at a high level.

We evaluated the time course of the effect of 1 mU/ml TSH on NOX4 and $p22^{phox}$ mRNA expression by real-time QPCR. Figure 2A shows that TSH increased the expression of these two genes in human thyrocytes. However, during TSH stimulation, $p22^{phox}$ mRNA levels showed greater variation (2- to 45-fold) at 48 h as compared with NOX4 mRNA levels (two- to four-fold). Western blot analysis showed that both NOX4 and $p22^{phox}$ protein levels increased after exposure to TSH, with a greater increase of $p22^{phox}$ protein level. NOX4 protein had an apparent molecular mass of 75 kDa, corresponding to its expected molecular weight (Wingler *et al*. 2001, Hilenski *et al*. 2004). Expression of the thyroid-specific protein TPO was shown as control (Fig. 2B). Because the NADPH oxidase NOX4 was described to play a role in superoxide and hydrogen peroxide production, we evaluated its contribution of increased intracellular ROS in TSH-stimulated thyrocytes. Figure 2C shows that TSH treatment for 48 h increased intracellular ROS levels (DCF fluorescence). Transfection of human thyrocytes with short interfering RNAs to NOX4 abolished the increase in intracellular ROS indicating that NOX4 was responsible for ROS generation elicited by TSH. Determination of the *NOX4* and $p22^{phox}$ mRNA levels in normal and tumor tissues was done by real-time QPCR. As shown in Fig. 3A, the expression levels of *NOX4* and $p22^{phox}$ mRNA varied only by eight- and five-fold among normal thyroid tissues respectively but by 54- and 95-fold among malignant thyroid tumors.

In benign thyroid tumors, *NOX4* and $p22^{phox}$ gene expression levels were not significantly different from those observed in normal thyroid tissues. However, the expression levels of *NOX4* and $p22^{phox}$ mRNA were significantly higher in all cancers than in normal tissues ($P=0.0006$ and $P=0.0136$). The increased *NOX4* expression level was significant in the PTC group ($P<0.0001$), and of borderline significance in FTC ($P=0.05$). In the 15-paired normal and tumor tissues (Fig. 3B), a significantly increased *NOX4* mRNA expression was found in tumors ($P=0.0006$).

The $p22^{phox}$ mRNA expression was significantly increased in the PTC and in ATC groups ($P=0.0031$ and $P=0.0257$), but differences between paired normal/tumor samples were not significant ($P=0.3028$). Finally, Fig. 4 shows that the expression of NOX4 and $p22^{phox}$ genes was significantly correlated ($r^2=0.425$; $P<0.0001$) in normal and in tumors tissues.

Expression of NOX4 protein was analyzed by immunohistochemistry (Fig. 5 and Table 2). NOX4 immunostained thyrocytes were found in all normal and pathological human thyroid specimens. In normal thyroid tissue, NOX4 immunostaining was intracytoplasmic and appeared granular on a faint diffuse positive background (Fig. 5A). Staining was clearly different to that of DUOX that is exclusively localized at the apical membrane (Fig. 5B). NOX4 immunostaining was heterogeneous. In the majority of cases, staining was present in activated tall columnar cells and absent in quiescent flat cells. Heterogeneity was found from one follicle to another and inside a given follicle (Fig. 5D). On serial sections immunostained for NOX4, CD34 (a vascular marker) and the NIS respectively NOX4 and NIS appeared positive in the same tall columnar cells and negative or weakly positive in flat cells. Positive cells were usually located in close contact with blood vessels (Fig. 5D–F).

In hyperplastic multinodular thyroid tissue, the same cell type heterogeneity was found. The so-called 'Sanderson pollsters' constituted of intraluminal papillary structures (Fig. 5C) and microfollicular structures budding from larger follicles were strongly stained. 'Sanderson pollsters' are accumulation of follicular cells in a small part of a follicle. This accumulation can be either solid or constituted by microfollicles. It is likely due to TSH stimulation heterogeneously distributed in thyroid follicles because variations of vascularization according to follicle area. At the subcellular level, NOX4 immunostaining was usually

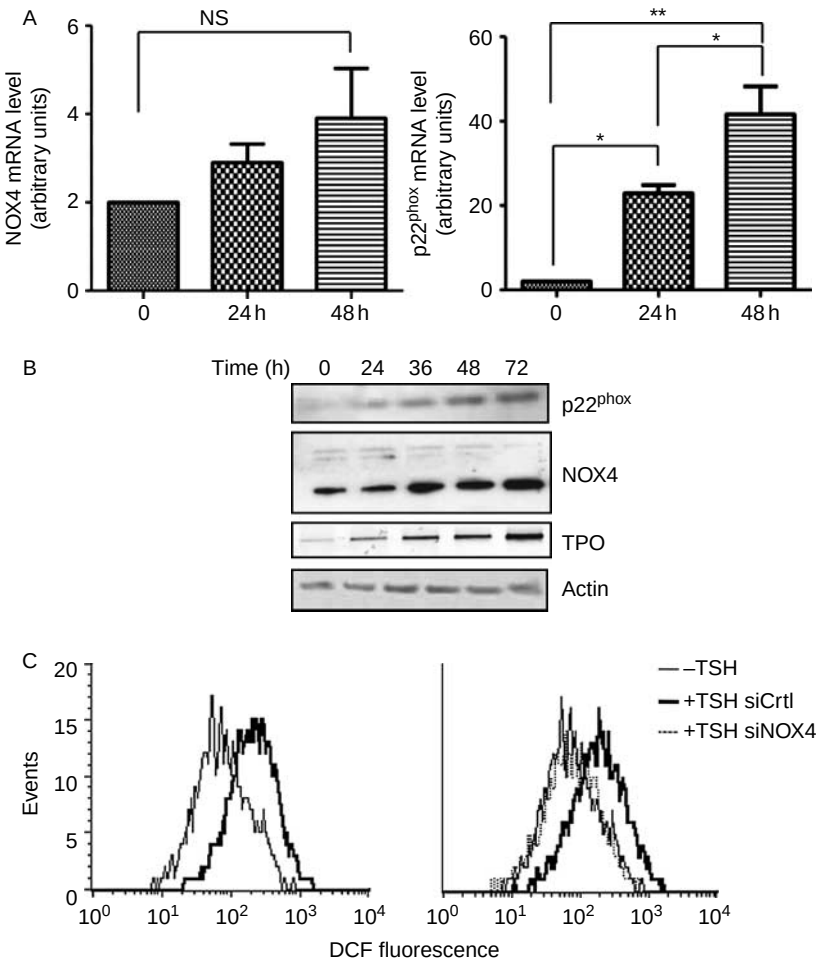

Figure 2 Effect of TSH on NOX4 and p22^{phox} expression in human thyrocytes. Primary human thyrocytes were maintained in 5H medium (without TSH) for 72 h and then incubated with 1 mU/ml TSH for the indicated periods. (A) Time-dependent stimulation of NOX4 and p22^{phox} transcription by TSH. mRNAs quantified by real-time RT-PCR were investigated in triplicates and expressed as means ± S.E.M. of one representative experiment from three independent cultures. Expression values (*y*-axis) are displayed on based 2 logarithmic scale. (B) Time-dependent stimulation of NOX4 and p22^{phox} protein expressions by TSH. NOX4 is recognized as a single band at 75 kDa by western blot analysis in human thyrocytes expressing the thyroperoxidase (TPO). Crude extracts of human thyrocytes were analyzed by western blotting. (C) Effect of TSH on NOX4-dependent ROS levels in human thyrocytes. ROS levels measured as DCF fluorescence by flow cytometry in human thyrocytes incubated for 48 h with or without 1 mU/ml TSH, and transiently transfected or not with short interfering RNAs to NOX4 as described in Materials and methods.

dispersed in the whole cytoplasm but in some cells it could be confined to the apical and/or basal cellular parts of the cytoplasm.

In follicular adenoma, heterogeneous staining was found, with a strong staining of the majority of small follicles (Fig. 5G).

In papillary carcinoma, immunostaining was homogeneous, being present in all malignant cells. Interestingly, staining was usually found at the apical and basal parts of the cytoplasm (Fig. 5H).

In poorly differentiated follicular carcinoma, NOX4 immunostaining was homogeneous, being present in all malignant cells. Staining was diffuse in the cytoplasm (Fig. 5I).

We also analyzed the expression of the integral membrane protein p22^{phox} and as expected, p22^{phox} displayed an identical cellular expression pattern and was also mainly present in the cytoplasm (Fig. 6). A strong immunoreactivity for p22^{phox} was also seen in macrophages, which contain the oxidase complex NOX2–p22^{phox} (Fig. 6D and F).

Discussion

A high concentration of ROS, resulting either from an increased production or/and from a reduced antioxidant activity, triggers an 'oxidative stress'. ROS are involved in several physiological processes, such as

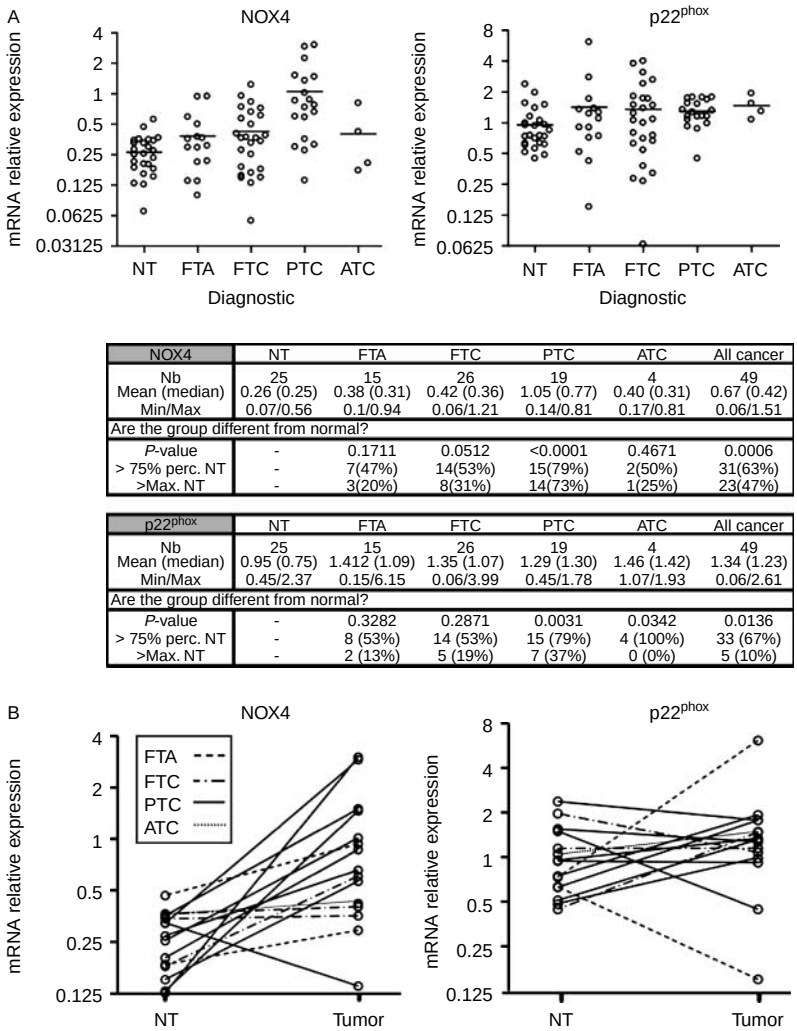

NOX4	NT	FTA	FTC	PTC	ATC	All cancer
Nb	25	15	26	19	4	49
Mean (median)	0.26 (0.25)	0.38 (0.31)	0.42 (0.36)	1.05 (0.77)	0.40 (0.31)	0.67 (0.42)
Min/Max	0.07/0.56	0.1/0.94	0.06/1.21	0.14/0.81	0.17/0.81	0.06/1.51
Are the group different from normal?						
P-value	-	0.1711	0.0512	<0.0001	0.4671	0.0006
> 75% perc. NT	-	7(47%)	14(53%)	15(79%)	2(50%)	31(63%)
>Max. NT	-	3(20%)	8(31%)	14(73%)	1(25%)	23(47%)

p22phox	NT	FTA	FTC	PTC	ATC	All cancer
Nb	25	15	26	19	4	49
Mean (median)	0.95 (0.75)	1.412 (1.09)	1.35 (1.07)	1.29 (1.30)	1.46 (1.42)	1.34 (1.23)
Min/Max	0.45/2.37	0.15/6.15	0.06/3.99	0.45/1.78	1.07/1.93	0.06/2.61
Are the group different from normal?						
P-value	-	0.3282	0.2871	0.0031	0.0342	0.0136
> 75% perc. NT	-	8 (53%)	14 (53%)	15 (79%)	4 (100%)	33 (67%)
>Max. NT	-	2 (13%)	5 (19%)	7 (37%)	0 (0%)	5 (10%)

Figure 3 Comparative expression of *NOX4* and *p22^{phox}* genes in human thyroid tissues analyzed by real-time quantitative reverse transcription PCR. Data are expressed as mRNA relative expression levels determined as X fold of calibrator corresponding to a pool of thyroid tissue samples and cell lines. Expression values (*y*-axis) are displayed on based 2 logarithmic scale. (A) Comparative expression of *NOX4* and *p22^{phox}* genes in several human thyroid tissue types: nontumoral (NT); follicular thyroid adenomas (FTA); follicular thyroid carcinomas (FTC); papillary thyroid carcinoma (PTC); and anaplastic thyroid carcinoma (ATC); (Table): distribution of mRNA relative expression levels of NOX4 and p22^{phox} according to the histological type. *Nb*, number of cases in each histological group; *Min/Max*, minimum and maximum of mRNA relative expression levels in each histological group l; *> 75%Perc.NT*, number of cases (percentage) displaying a mRNA relative expression level higher than the 75% percentile expression level of normal tissues; *> Max of NT*, number of cases (percentage) displaying a mRNA relative expression level higher than the higher expression level in normal tissues. (B) Comparative expression of NOX4 and p22^{phox} genes in 15 paired samples of normal and tumor tissues. (NT, paired normal counterpart; T, tumors, corresponding to 2 (FTA), 3 FTC, 9 PTC, and 1 ATC. Each value represents the mRNA relative expression level.

host defense, cell growth, differentiation, protein synthesis, and angiogenesis (Bedard & Krause 2007, Lambeth 2007, Mittal *et al*. 2007). ROS are seen as intra- and extracellular messengers with a tightly controlled production. This concept was reinforced by the discovery of six NOXes, with the presence of several NOXes in the same cells, suggesting different intracellular H_2O_2-producing compartments with specific functions (Hilenski *et al*. 2004).

In this study, for the first time, we demonstrate the presence of NOX4 and its partner p22^{phox} that is required for its catalytic activity and forms a heterodimeric enzyme complex with NOX4 and, that is localized and produces ROS inside the thyroid cell. TSH stimulation increases ROS production by thyrocytes in culture and siRNA to NOX4 prevent the increase in intracellular ROS, indicating that NOX4 was responsible for ROS generation. Importantly, we

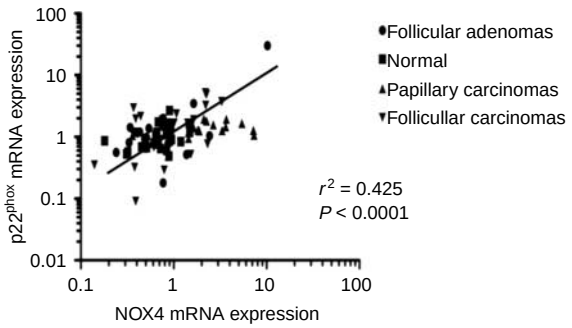

Figure 4 Correlation between NOX4 and $p22^{phox}$ mRNA levels in normal and tumor tissues. Correlation between expression profiles was studied using Spearman's rank-order correlation coefficient. The level of significance chosen was 5%.

found that NOX4 and $p22^{phox}$ expressions are both positively regulated by TSH, with a highest regulation for $p22^{phox}$, which is known to stabilize and increase NOX4 at the protein level (Ambasta *et al*. 2004). This result suggests a role for ROS in TSH signaling, which is mediated through NOX4.

Its intracellular localization probably corresponds to the endoplasmic reticulum where it was recently found in other cell types (Chen *et al*. 2008). This localization also suggests a role of NOX4 in cell signaling, unlike DUOX which are only active at the apical cell surface of thyrocytes where they produce H_2O_2 in the extracellular colloid space. Furthermore, thyroid cells possess very potent H_2O_2 degradation systems, which prevent the intracytoplasmic diffusion of extracellular H_2O_2 and intracellular iodide organification (Björkman & Ekholm 1995, Ekholm & Björkman 1997). The strong NOX4 staining in activated columnar thyrocytes and in their hyperplastic protrusion in the follicular lumen suggests a relationship with proliferation and functional activity. The presence of NOX4 in solid cell aggregation or microfollicles budding from larger follicles might be related with follicle replication. Basal localization of NOX4 in close relation with blood vessels could be in agreement with the described angiogenic properties of NOX4, through HIF-1 and VEGF (Xia *et al*. 2007). NOX4 was

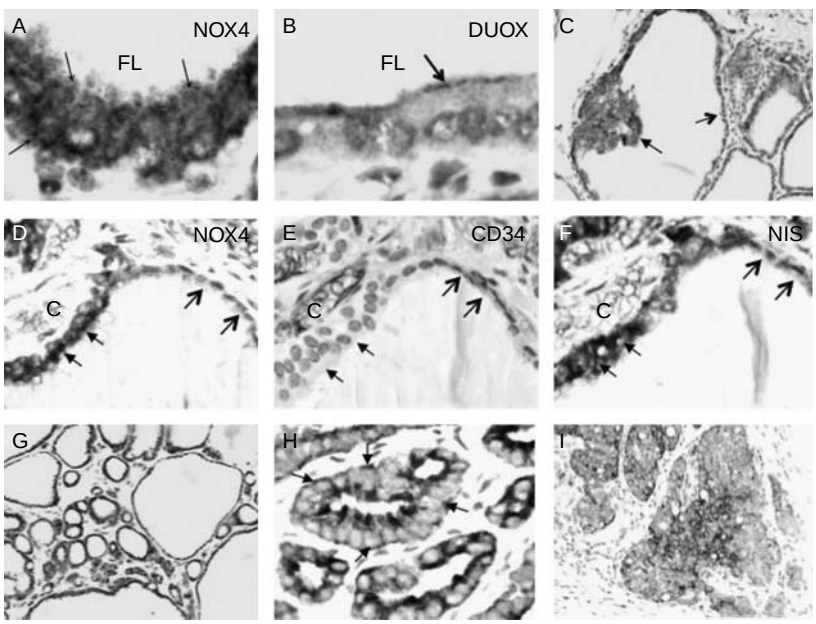

Figure 5 NOX4 protein expression in human thyroid tissues. (A) normal thyroid tissue. Note intracytoplasmic granular staining of NOX4 (arrows) on a diffusely stained background; FL, follicular lumen; magnification, ×1000. (B) DUOX immunostaining is essentially localized at the apical membrane (arrow). Note faint, diffuse, intracytoplasmic staining. FL, follicular lumen. Magnification, ×1000. (C) follicular hyperplasia. NOX4-positive intraluminal so-called 'Sanderson pollster' (solid arrow). Note negative flat quiescent cells in the same follicle (thin arrow). Magnification, ×200. (D–F) NOX4, CD34 and NIS immunostainings on serial sections from the same follicle at the junction of activated columnar cells (solid arrows) and flat quiescent cells (thin arrows). Note on (E) that activated columnar cells are pseudostratified and present nuclei much larger than flat cells. Moreover, these cells are in contact to vessel endothelium, in contrast to flat cells. NOX4 and NIS display a strong immunostaining in large activated cells (solid arrows), and a negative or weak signal in quiescent flat cells (thin arrows). In vessels, red blood cells display pseudo-peroxidase activity, which has not been removed. Magnification, ×400. (G) Follicular thyroid adenoma. Small follicles present a larger number of NOX4-positive cells than macrofollicles. Magnification, ×200. (H) Papillary carcinoma. All tumor cells are NOX4 positive. Most staining is localized at the apical side, but some staining can be seen at the basal part (arrows). Magnification, ×400. (I) Poorly differentiated follicular carcinoma. Diffuse staining is seen in all tumor cells. Magnification, ×200.

Table 2 Relationship between clinicopathologic characteristics of the thyroid tissues studied and percentage of NOX4-immunostained cells in the thyroid samples

	n	<25%	25–50%	50–75%	>75%
Normal	8	0	2	6	0
Nodular hyperplasia	11	0	1	9	1
Follicular adenoma	4	2	0	2	0
Papillary carcinoma	11	0	1	4	6
Follicular carcinoma	3	0	0	0	3
P. D. F. C.	4	0	0	0	4

originally identified as a NOX homolog highly expressed in the kidney and has been postulated to be involved in oxygen sensing (Geiszt *et al*. 2000, Shiose *et al*. 2001).

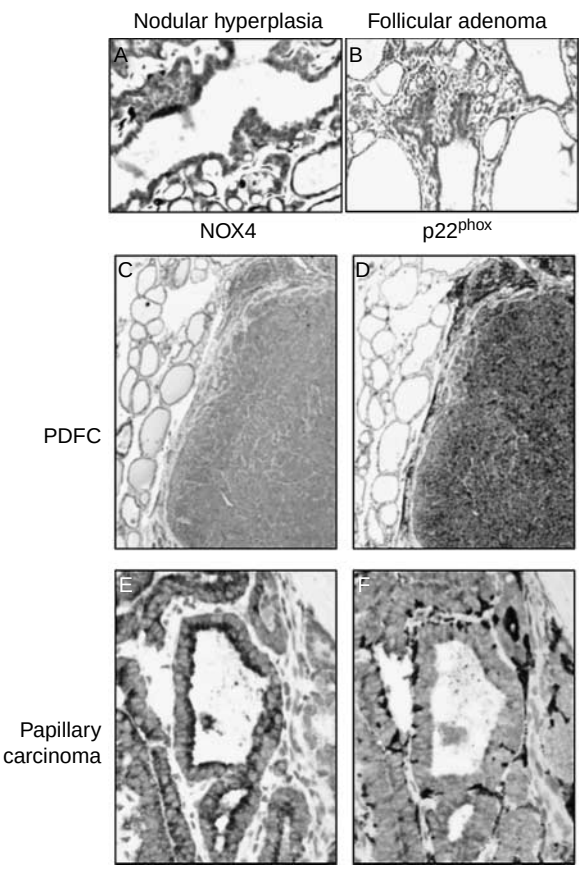

Figure 6 p22^{phox} protein expression in human thyroid tissues. (A) Thyroid nodular hyperplasia. As observed for NOX4, staining of p22^{phox} is heterogeneous. Magnification, ×200. (B) Follicular thyroid adenoma. p22^{phox} immunostaining is essentially localized in activated columnar cells. Magnification, ×100. (C–F) NOX4 and p22^{phox} immunostaining on serial sections from the same tumoral region in poorly differentiated follicular carcinoma (PDFC) (magnification ×100) and in papillary thyroid carcinoma (magnification ×400) respectively. All tumor cells are positive and display the same staining profile. Note a strong p22^{phox} immunostaining in macrophages corresponding to the expression of the NOX2–p22^{phox} complex.

NOX4 was shown to produce H_2O_2 continuously (Geiszt *et al*. 2000), and *in vivo* increased activity was linked to elevated mRNA levels (Gorin *et al*. 2003). ROS are overproduced in cancer cells (Quinn *et al*. 2006, Lambeth 2007), and inhibitors of NOX decrease cell proliferation (Brar *et al*. 2002). Furthermore, NOX4 increases survival properties in pancreatic cancer cells (Edderkaoui *et al*. 2005). Importantly, we observed in this study that NOX4 and p22^{phox} mRNA were up-regulated in thyroid cancers, particularly in papillary thyroid cancers, suggesting that this H_2O_2-generating system could be involved in the signaling mechanism in thyroid tumor cells. As shown by immunohistochemistry, NOX4 is specifically expressed at a high level in thyrocytes, unlike p22^{phox}, which is highly expressed also in macrophages. This could explain the absence of differences observed for p22^{phox} expression between paired normal/tumor samples.

An imbalance between the production of ROS and degradation leads to oxidative stress, which can damage cell components, including proteins, lipids, and DNA. Interestingly, in mice, the spontaneous mutation frequency is higher in the thyroid gland as compared with other organs (Maier *et al*. 2006). In human thyroid tissues, there is also a high frequency of somatic mutations of the TSH receptor (Krohn *et al*. 2007). Until now, DUOX1 and DUOX2, as the only known H_2O_2-generating systems in the thyroid gland, were suspected to play a role in the mutagenesis in the thyroid gland, in particular under conditions of iodine and selenium deficiency (Song *et al*. 2007). The discovery of NOX4 expression in the thyroid gland and its intracytoplasmic localization open new avenues of research concerning the role of the NOX4-derived ROS in TSH signaling and in the mechanisms leading to oxidative stress, genetic instability, and mutagenesis that might contribute to the development and progression of thyroid tumors.

Declaration of interest

The authors declare that there are no conflicts of interest that would prejudice the impartiality of this study.

Funding

This work was supported by grants from Association pour la Recherche sur le Cancer (ARC) (grant number 3945), Agence Nationale de la Recherche (ANR) (grant number 238503), Ligue Contre le Cancer (comité du Val-de-Marne), and Electricité de France (EDF).

Author contribution statement

Urbain Weyemi and Bernard Caillou contributed equally to this study.

References

Ambasta RK, Kumar P, Griendling KK, Schmidt HH, Busse R & Brandes RP 2004 Direct interaction of the novel Nox proteins with $p22^{phox}$ is required for the formation of a functionally active NADPH oxidase. *Journal of Biological Chemistry* **279** 45935–45941.

Ameziane-El-Hassani R, Morand S, Boucher JL, Frappart YM, Apostolou D, Agnandji D, Gnidehou S, Ohayon R, Noel-Hudson MS, Francon J *et al.* 2005 Dual oxidase-2 has an intrinsic Ca^{2+}-dependent H_2O_2-generating activity. *Journal of Biological Chemistry* **280** 30046–30054.

Babior BM 1999 NADPH oxidase: an update. *Blood* **93** 1464–1476.

Bedard K & Krause KH 2007 The NOX family of ROS-generating NADPH oxidases: physiology and pathophysiology. *Physiological Reviews* **87** 245–313.

Björkman U & Ekholm R 1995 Hydrogen peroxide degradation and glutathione peroxidase activity in cultures of thyroid cells. *Molecular and Cellular Endocrinology* **111** 99–107.

Brar SS, Kennedy TP, Sturrock AB, Huecksteadt TP, Quinn MT, Whorton AR & Hoidal JR 2002 An NAD(P)H oxidase regulates growth and transcription in melanoma cells. *American Journal of Physiology. Cell Physiology* **282** C1212–C1224.

Caillou B, Dupuy C, Lacroix L, Nocera M, Talbot M, Ohayon R, Deme D, Bidart JM, Schlumberger M & Virion A 2001 Expression of reduced nicotinamide adenine dinucleotide phosphate oxidase (ThoX, LNOX, Duox) genes and proteins in human thyroid tissues. *Journal of Clinical Endocrinology and Metabolism* **86** 3351–3358.

Chen K, Kirber MT, Xiao H, Yang Y & Keaney JF Jr 2008 Regulation of ROS signal transduction by NADPH oxidase 4 localization. *Journal of Cell Biology* **181** 1129–1139.

De Deken X, Wang D, Many MC, Costagliona S, Libert F, Vassart G, Dumont JE & Miot F 2000 Cloning of two human thyroid cDNAs encoding new members of the NADPH oxidase family. *Journal of Biological Chemistry* **275** 23227–23233.

Dupuy C, Ohayon R, Valent A, Noel-Hudson MS, Deme D & Virion A 1999 Purification of a novel flavoprotein involved in the thyroid NADPH oxidase. Cloning of the porcine and human cDNAs. *Journal of Biological Chemistry* **274** 37265–37269.

Duthoit C, Estienne V, Giraud A, Durand-Gorde JM, Rasmussen AK, Feldt-Rasmussen U, Carayon P & Ruf J 2001 Hydrogen peroxide-induced production of a 40 kDa immunoreactive thyroglobulin fragment in human thyroid cells: the onset of thyroid autoimmunity? *Biochemical Journal* **360** 557–562.

Edderkaoui M, Hong P, Vaquero EC, Lee JK, Fischer L, Friess H, Buchler MW, Lerch MM, Pandol SJ & Gukovskaya AS 2005 Extracellular matrix stimulates reactive oxygen species production and increases pancreatic cancer cell survival through 5-lipoxygenase and NADPH oxidase. *American Journal of Physiology. Gastrointestinal and Liver Physiology* **289** G1137–G1147.

Ekholm R & Björkman U 1997 Glutathione peroxidase degrades intracellular hydrogen peroxide and thereby inhibits intracellular protein iodination in thyroid epithelium. *Endocrinology* **138** 2871–2878.

Geiszt M, Kopp JB, Várnai P & Leto TL 2000 Identification of renox, an NAD(P)H oxidase in kidney. *PNAS* **97** 8010–8014.

Gorin Y, Ricono JM, Kim NH, Bhandari B, Choudhury GG & Abboud HE 2003 Nox4 mediates angiotensin II-induced activation of Akt/protein kinase B in mesangial cells. *American Journal of Physiology. Renal Physiology* **285** F219–F229.

Hilenski LL, Clempus RE, Quinn MT, Lambeth JD & Griendling KK 2004 Distinct subcellular localizations of Nox1 and Nox4 in vascular smooth muscle cells. *Arteriosclerosis, Thrombosis, and Vascular Biology* **24** 677–683.

Krohn K, Maier J & Paschke R 2007 Mechanisms of disease: hydrogen peroxide, DNA damage and mutagenesis in the development of thyroid tumors. *Nature Clinical Practice. Endocrinology & Metabolism* **3** 713–720.

Lacroix L, Lazar V, Michiels S, Ripoche H, Dessen P, Talbot M, Caillou B, Levillain JP, Schlumberger M & Bidart JM 2005 Follicular thyroid tumors with the PAX8–PPAR-gamma1 rearrangement display characteristic genetic alterations. *American Journal of Pathology* **167** 223–231.

Lambeth JD 2007 Nox enzymes, ROS, and chronic disease: an example of antagonistic pleiotropy. *Free Radical Biology & Medicine* **43** 332–347.

Maier J, van Steeg H, van Oostrom C, Karger S, Pashke R & Krohn K 2006 Deoxyribonucleic acid damage and spontaneous mutagenesis in the thyroid gland of rats and mice. *Endocrinology* **147** 3391–3397.

Mittal M, Roth M, König P, Hofmann S, Dony E, Goyal P, Selbitz AC, Schermuly RT, Ghofrani HA, Kwapiszewska G *et al.* 2007 Hypoxia-dependent regulation of nonphagocytic NADPH oxidase subunit NOX4 in the pulmonary vasculature. *Circulation Research* **101** 258–267.

Morand S, Chaaraoui M, Kaniewski J, Dème D, Ohayon R, Noel-Hudson MS, Virion A & Dupuy C 2003 Effect of

iodide on nicotinamide adenine dinucleotide phosphate oxidase activity and Duox2 protein expression in isolated porcine thyroid follicles. *Endocrinology* **144** 1241–1248.

Pomerance M, Abdullah HB, Kamerji S, Correze C & Blondeau JP 2000 Thyroid-stimulating hormone and cyclic AMP activate p38 mitogen-activated protein kinase cascade. Involvement of protein kinase A, rac1, and reactive oxygen species. *Journal of Biological Chemistry* **275** 40539–40546.

Quinn MT, Ammons MC & Deleo FR 2006 The expanding role of NADPH oxidases in health and disease: no longer just agents of death and destruction. *Clinical Science* **111** 1–20.

Shiose A, Kuroda J, Tsuruya K, Hirai M, Hirakata H, Naito S, Hatorri M, Sakaki Y & Sumimoto HA 2001 Novel superoxide-producing NAD(P)H oxidase in kidney. *Journal of Biological Chemistry* **276** 1417–1423.

Song Y, Driessens N, Costa M, De Deken X, Detours V, Corvilain B, Maenhaut C, Miot F, Van Sande J, Many MC *et al.* 2007 Roles of hydrogen peroxide in thyroid physiology and disease. *Journal of Clinical Endocrinology and Metabolism* **92** 3764–3773.

Vandesompele J, De Preter K, Pattyn F, Poppe B, Van Roy N, De Paepe A & Speleman F 2002 Accurate normalization of real-time quantitative RT-PCR data by geometric averaging of multiple internal control genes. *Genome Biology* **3** 1–11.

Verhoeven AJ, Bolscher BG, Meerhof LJ, van Zwieten R, Keijer J, Weening RS & Roos D 1989 Characterization of two monoclonal antibodies against cytochrome b558 of human neutrophils. *Blood* **73** 1686–1694.

Wang D, De Deken X, Milenkovic M, Song Y, Pirson I, Dumont JE & Miot F 2005 Identification of a novel partner of duox: EFP1, a thioredoxin-related protein. *Journal of Biological Chemistry* **280** 3096–3103.

Wingler K, Wünsch S, Kreutz R, Rothermund L, Paul M & Schmidt HH 2001 Upregulation of the vascular NAD(P)H-oxidase isoforms Nox1 and Nox4 by the renin–angiotensin system *in vitro* and *in vivo*. *Free Radical Biology & Medicine* **31** 1456–1464.

Xia C, Meng Q, Liu LZ, Rojanasakul Y, Wang XR & Jiang BH 2007 Reactive oxygen species regulate angiogenesis and tumor growth through vascular endothelial growth factor. *Cancer Research* **67** 10823–10830.